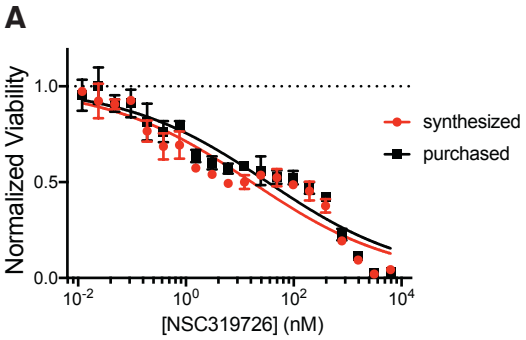

95% CI of EC_{50}
synthesized: 11.15 to 24.70 nM
purchased: 21.47 to 47.02 nM

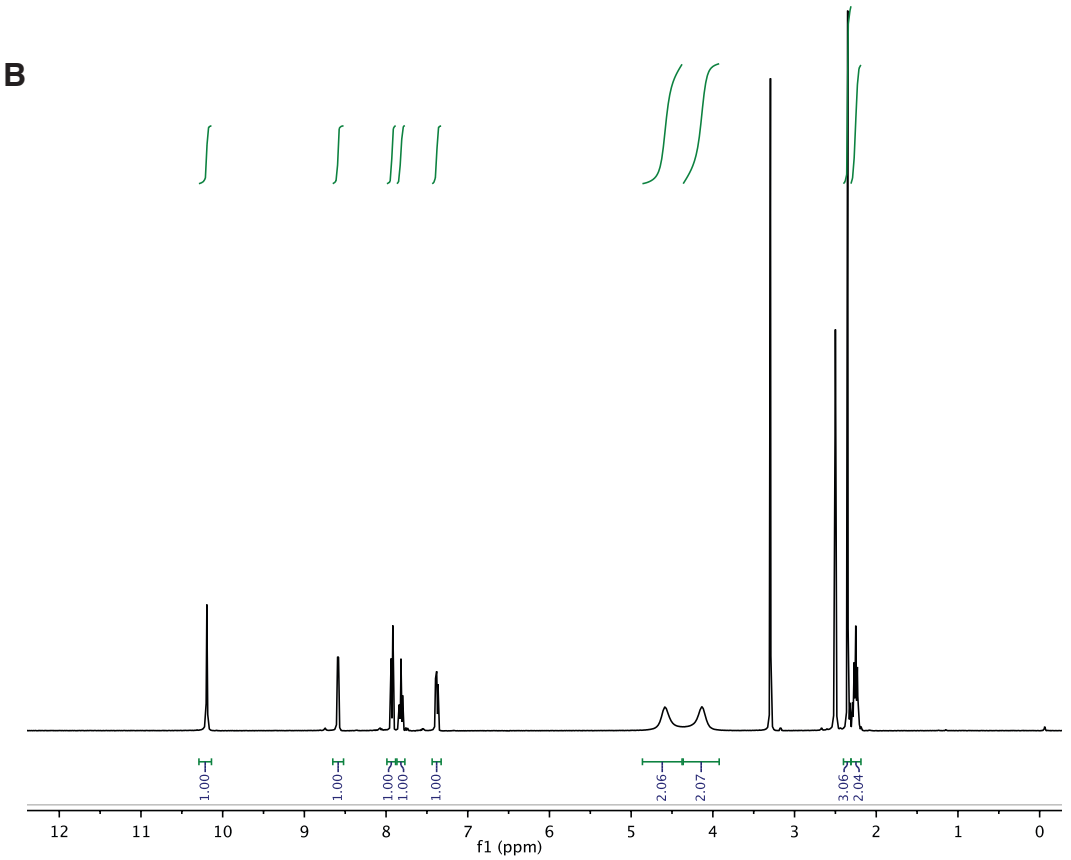

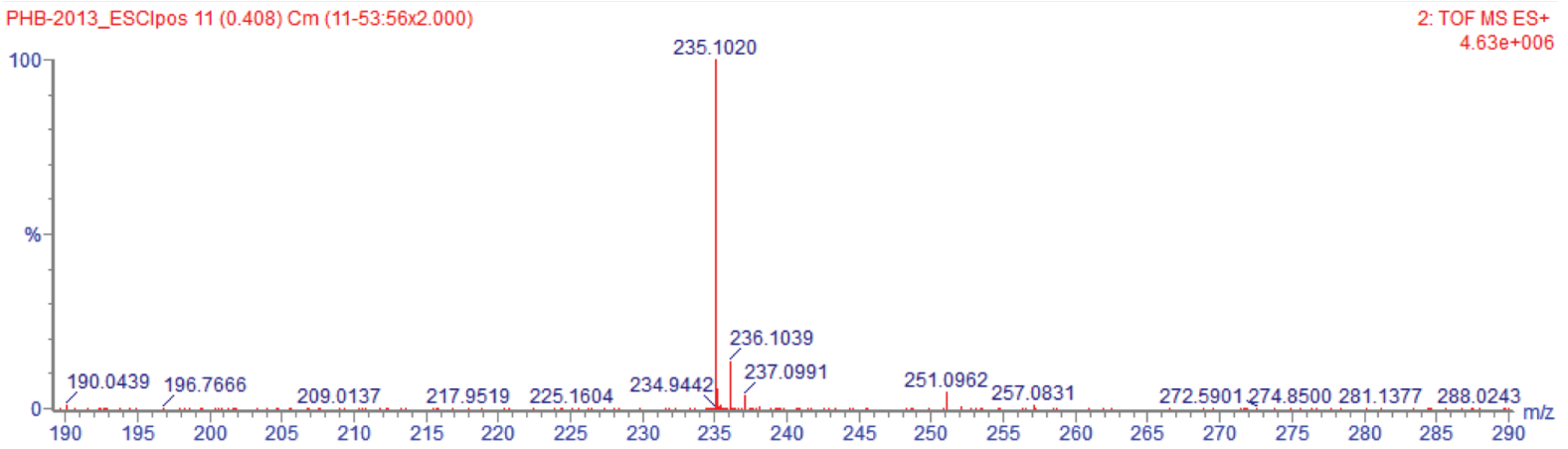

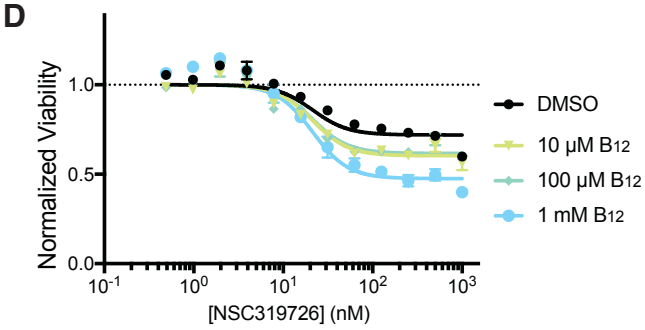

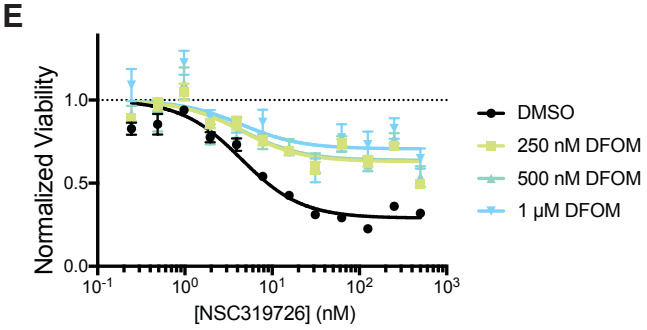

Figure S1. Quality of synthesized NSC319726 and effects of metals on its lethality confirmed, related to Figure 1.

A. Comparison of potencies between synthesized and purchased NSC319726 in HF2941 GBM cells. **B.** ^{1}H NMR spectrum of synthesized NSC319726 (in-house ID: PHB2013) in DMSO-*d6*. **C.** High-res mass spec of synthesized NSC319726. **D.** Effect of various concentrations of holo Vitamin B_{12} supplementation on sensitivity to NSC319726 in HT-1080 cells. **E.** Effect of various concentrations of an iron-chelator deferoxamine (DFOM) cotreatment on sensitivity to NSC319726 in HT-1080 cells. Dose curves in **A, D,** and **E** show mean ± SEM of technical triplicates.

A

Criteria	Pro-death pathways (agonizing NSC319726)	Pro-survival pathways (antagonizing NSC319726)
i) Correlation across the NCI-60 panel	More expressed in sensitive cells	More expressed in resistant cells
ii) Cellular response of GBM upon NSC treatment	Down-regulated upon NSC treatment	Up-regulated upon NSC treatment

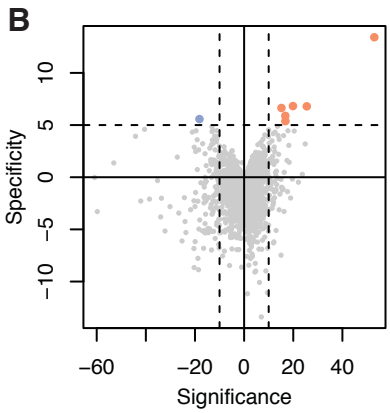

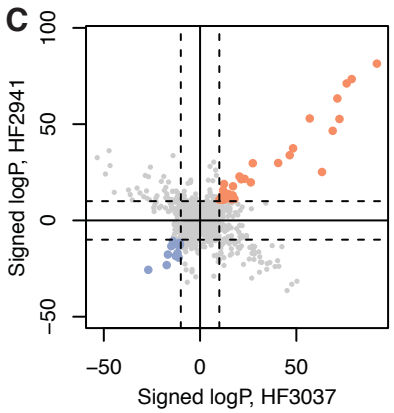

D

	NCI60 pharmacogenomics			GBM transcriptome upon ZMC1 treatment			
Pathway Name	Significance	Specificity	is.selected (NCI)	Basal	diff.exp. (hf3037)	diff.exp (hf2941)	is.selected (GBM)
HALLMARK_TNFA_SIGNALING_VIA_NFKB	25.51	6.80	TRUE	12.08	63.33	25.18	TRUE
HALLMARK_HYPOXIA	16.76	5.89	TRUE	7.08	48.30	37.49	TRUE
KEGG_OLFACTORY_TRANSDUCTION	-2.61	-1.88	FALSE	-61.28	71.30	63.38	TRUE
PID_P53_DOWNSTREAM_PATHWAY	3.84	-1.31	FALSE	2.01	12.44	18.95	TRUE
PID_HIF1_TFPATHWAY	3.53	-0.79	FALSE	3.45	14.62	13.57	TRUE
REACTOME_DEFENSINS	1.26	-0.86	FALSE	-9.58	11.40	10.88	TRUE
REACTOME_SIGNALING_BY_GPCR	7.61	-3.24	FALSE	34.27	40.56	29.86	TRUE
REACTOME_OLFACTORY_SIGNALING_PATHWAY	-1.84	-2.75	FALSE	-71.16	76.13	71.16	TRUE
REACTOME_GPCR_DOWNSTREAM_SIGNALING	7.09	-3.57	FALSE	37.93	46.56	33.91	TRUE
GO_NEGATIVE_REGULATION_OF_GENE_EXPRESSION	-3.11	-1.50	FALSE	8.00	10.03	10.78	TRUE
GO_CELL_DEATH	4.68	0.98	FALSE	8.09	16.21	11.00	TRUE
GO_SINGLE_ORGANISM_BIOSYNTHETIC_PROCESS	-5.56	-5.78	FALSE	-3.25	-11.69	-16.94	TRUE
GO_SENSORY_PERCEPTION_OF_CHEMICAL_STIMULUS	3.73	-1.90	FALSE	-65.46	78.76	73.43	TRUE
GO_ORGANOPHOSPHATE_METABOLIC_PROCESS	-2.15	-6.93	FALSE	2.18	-10.70	-11.62	TRUE
GO_POSITIVE_REGULATION_OF_GENE_EXPRESSION	-1.92	-4.60	FALSE	14.64	12.10	10.70	TRUE
GO_CARBOHYDRATE_DERIVATIVE_METABOLIC_PROCESS	2.63	-7.79	FALSE	2.29	-11.11	-19.30	TRUE
GO_NUCLEOBASE_CONTAINING_SMALL_MOLECULE_METABOLIC_PROCESS	-5.75	-1.14	FALSE	2.41	-14.13	-10.78	TRUE
GO_RESPONSE_TO_OXYGEN_LEVELS	6.07	-1.57	FALSE	5.46	14.40	13.78	TRUE
GO_G_PROTEIN_COUPLED_RECEPTOR_SIGNALING_PATHWAY	7.97	-3.49	FALSE	44.05	68.88	46.57	TRUE
GO_RESPONSE_TO_ABIOTIC_STIMULUS	3.24	-2.50	FALSE	5.89	14.10	13.30	TRUE
GO_RIBONUCLEOPROTEIN_COMPLEX_BIOGENESIS	-44.22	3.93	FALSE	6.02	15.43	13.35	TRUE
GO_DETECTION_OF_STIMULUS	2.66	-2.28	FALSE	-48.27	56.97	52.98	TRUE
GO_GLYCOSYL_COMPOUND_METABOLIC_PROCESS	-6.77	-0.82	FALSE	2.36	-10.86	-13.03	TRUE
GO_MRNA_METABOLIC_PROCESS	-35.24	-0.32	FALSE	7.70	11.16	12.39	TRUE
GO_PROTEIN_COMPLEX_SUBUNIT_ORGANIZATION	-8.22	2.30	FALSE	-6.26	-12.10	-12.41	TRUE
GO_CELLULAR_RESPONSE_TO_STRESS	-4.75	-0.88	FALSE	-7.85	27.40	29.73	TRUE
GO_REGULATION_OF_TRANSCRIPTION_FROM_RNA_POLYMERASE_II_PROMOTER	1.70	-3.46	FALSE	13.08	13.31	12.99	TRUE
GO_INTERMEDIATE_FILAMENT	1.30	-3.18	FALSE	-14.21	17.11	17.77	TRUE
GO_ORGANELLE_INNER_MEMBRANE	-21.08	4.33	FALSE	-9.23	-16.70	-17.68	TRUE
GO_MITOCHONDRIAL_MATRIX	-15.99	-0.58	FALSE	-8.28	-10.42	-12.52	TRUE
GO_MITOCHONDRIAL_PART	-24.04	-4.24	FALSE	-15.60	-17.32	-23.16	TRUE
GO_MITOCHONDRION	-19.94	-6.17	FALSE	-18.89	-26.88	-25.63	TRUE
GO_INTERMEDIATE_FILAMENT_CYTOSKELETON	1.43	-1.60	FALSE	-11.54	11.93	15.65	TRUE
GO_KERATIN_FILAMENT	2.11	-2.61	FALSE	10.37	16.99	13.02	TRUE
GO_ENVELOPE	-19.10	3.60	FALSE	-14.69	-14.94	-13.35	TRUE
GO_MITOCHONDRIAL_ENVELOPE	-17.62	-0.53	FALSE	-10.90	-12.64	-18.45	TRUE
GO_OLFACTORY_RECEPTOR_ACTIVITY	-2.05	-3.09	FALSE	-79.97	91.83	81.46	TRUE
GO_G_PROTEIN_COUPLED_RECEPTOR_ACTIVITY	7.68	0.40	FALSE	53.35	72.41	52.71	TRUE
GO_ENZYME_BINDING	4.78	-2.26	FALSE	7.16	17.86	11.22	TRUE
GO_POLY_A_RNA_BINDING	-60.85	-0.02	FALSE	-11.50	20.46	22.83	TRUE
GO_RNA_BINDING	-59.76	-3.29	FALSE	-12.20	21.36	21.41	TRUE
GO_ODORANT_BINDING	NA	NA	FALSE	-19.78	23.15	21.62	TRUE
HALLMARK_GLYCOLYSIS	5.43	-1.10	FALSE	5.61	14.31	11.54	TRUE
HALLMARK_P53_PATHWAY	3.75	-0.95	FALSE	3.22	26.37	19.78	TRUE
GO_REGULATION_OF_ANATOMICAL_STRUCTURE_MORPHOGENESIS	19.87	6.83	TRUE	11.63	-6.30	-9.64	FALSE
GO_NEGATIVE_REGULATION_OF_RESPONSE_TO_STIMULUS	15.20	6.64	TRUE	9.86	10.32	-4.79	FALSE
GO_NUCLEAR_CHROMOSOME_TELOMERIC_REGION	-18.17	5.58	TRUE	-2.25	-4.20	3.86	FALSE
GO_GOLGI_APPARATUS	16.81	5.38	TRUE	-10.33	10.73	-14.50	FALSE
HALLMARK_EPITHELIAL_MESENCHYMAL_TRANSITION	52.99	13.42	TRUE	32.47	7.37	-18.27	FALSE

Figure S2. Pharmacogenomic analysis of NSC319726's mechanism of action, related to Figure 4.
A. Criteria for choosing pathways involved in NSC319726-induced cell death. **B.** Pathways (gene sets) predicted to be involved in NSC319726's mechanism of action (MoA) through NCI-60 pharmacogenomics. Each point corresponds to one pathway (gene set), whose x- and y-coordinates correspond to significance and specificity. Orange points are expected to be pro-survival pathways while blue points are expected to be pro-death pathways. **C.** Pathways predicted to be involved in NSC319726's MoA through RNA-seq of GBM cells treated with NSC319726. x- and y- coordinates correspond to signed logP values in HF3037 (most sensitive) and HF2941 (most resistant) GBM cells. Color codes are the same as in **B. D.** Pathways that were significantly associated with NSC319726's mechanism of action either in **B** or **C** are shown on this list.

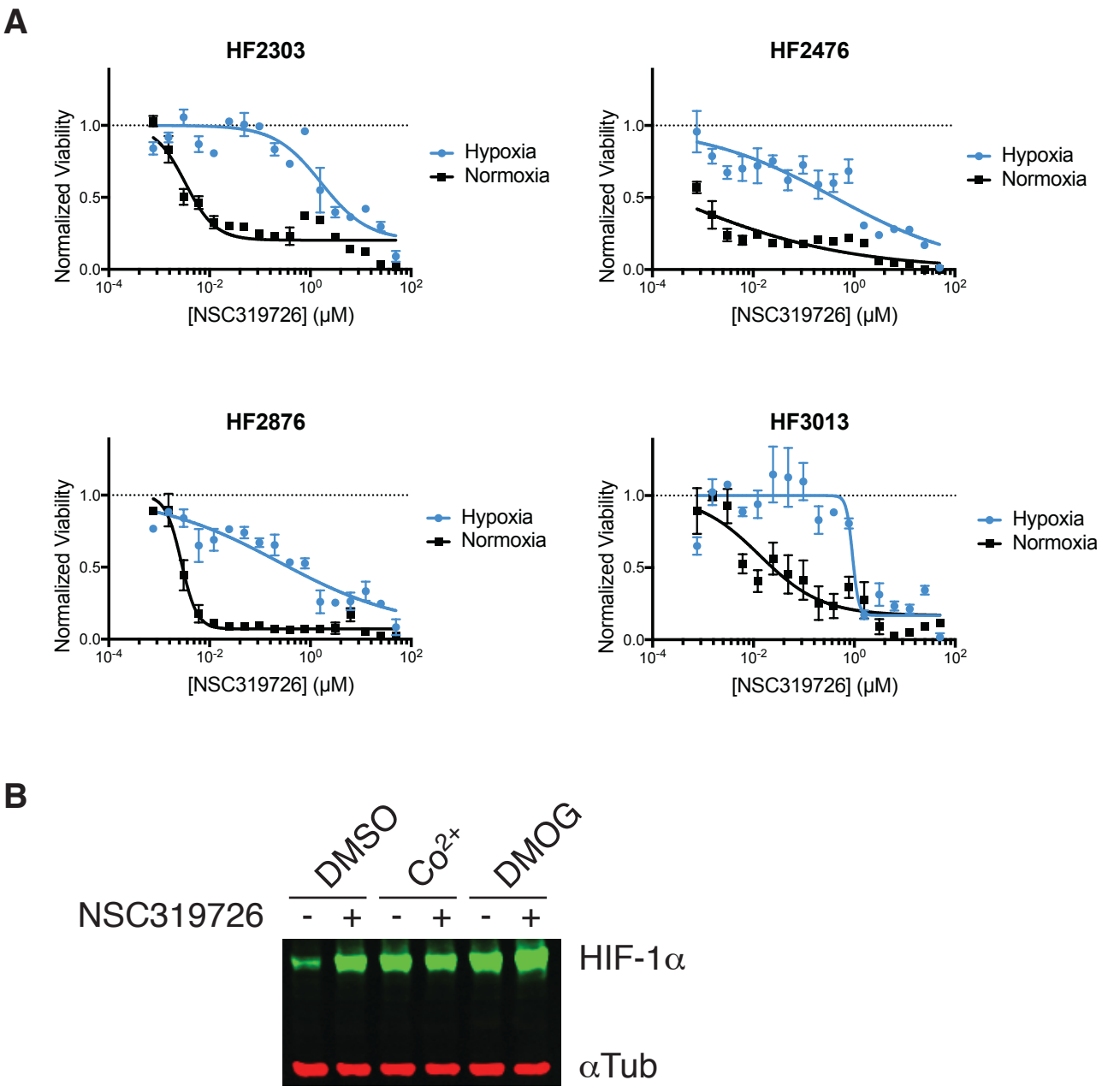

Figure S3. NSC319726's mechanism of action and hypoxia, related to Figure 4.
A. Sensitivity to NSC319726 in four GBM cells under normoxia and hypoxia. **B.** Pharmacological stabilization of HIF-1α. Dose curves in **A** show mean ± SEM of technical triplicates.

A HF3037

		DOWN	
		consistent	not
UP	consistent	27	64
	not	40	799

B HF2941

		DOWN	
		consistent	not
UP	consistent	14	45
	not	30	841

C Consistent experiments with two cell lines

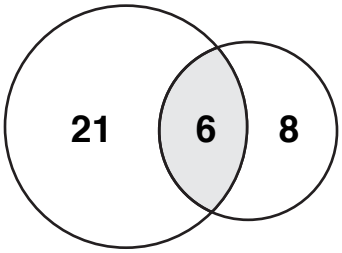

	HF3037		HF2941	
	UP	DOWN	UP	DOWN
BUYTAERT_PHOTODYNAMIC_THERAPY_STRESS	163.39	-86.37	62.49	-24.30
BLALOCK_ALZHEIMERS_DISEASE	30.71	-25.51	12.55	-25.79
GRAESSMANN_APOPTOSIS_BY_DOXORUBICIN	29.90	-52.85	16.02	-19.87
CONCANNON_APOPTOSIS_BY_EPOXOMICIN	28.07	-22.03	12.25	-12.56
SENESE_HDAC1_TARGETS	20.10	-16.39	20.10	-21.67
RODRIGUES_THYROID_CARCINOMA_ANAPLASTIC	18.82	-14.19	26.89	-19.14

D Up/down-regulated genes in Buytaert *et al*.

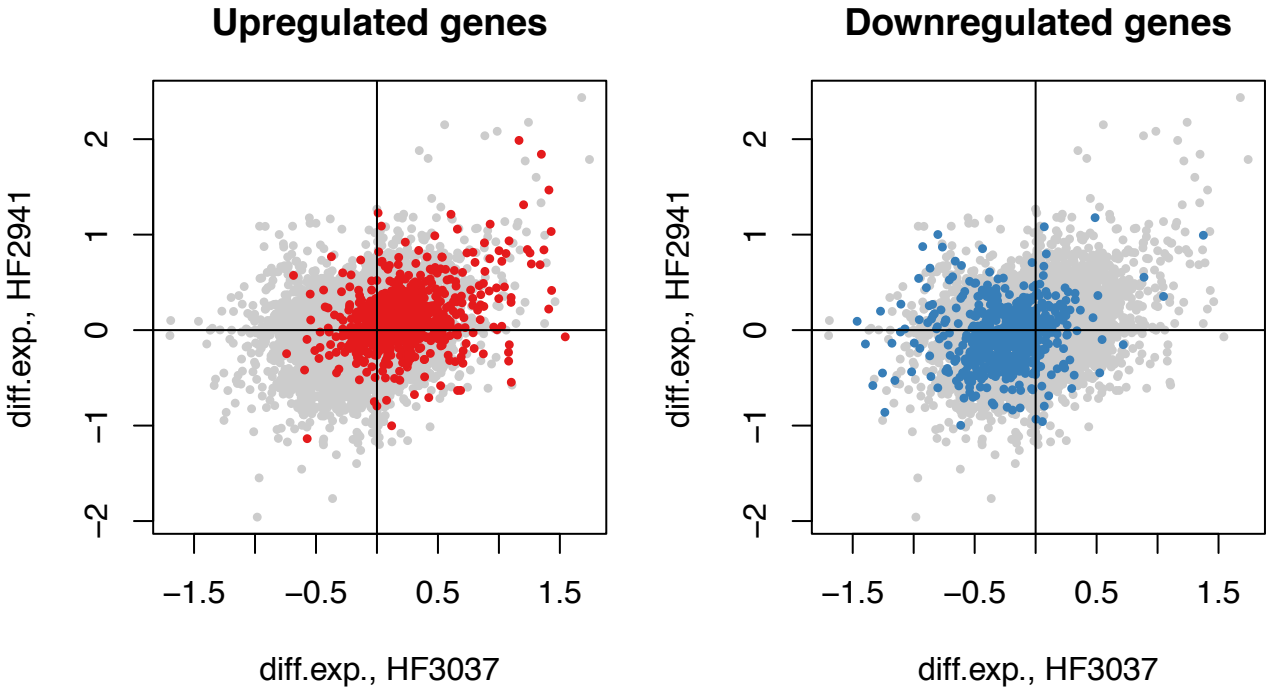

Figure S4. Experiments inducing similar gene expression changes to NSC treatment, related to Figure 5. **A.** Contingency table showing the number of experimental conditions from MSigDB whose gene expression changes are consistent in HF3037 cells. Both up- and down-regulated gene sets of each experiment were compiled in MSigDB. An experiment was considered consistent when genes up- or down-regulated in the experiment were also significantly changed in the same way upon NSC319726 treatment in the cells. **B.** Contingency table in HF2941 cells. **C.** 6 experiments were consistent regarding both up- and down-regulated genes in both HF3037 and HF2941 cells. **D.** Scatter plots showing log10-fold changes of gene expression upon NSC319726 over DMSO treatments in the two GBM cells. Up- and down-regulated genes in Buytaert *et al.* were colored in red and blue in the plots, respectively.

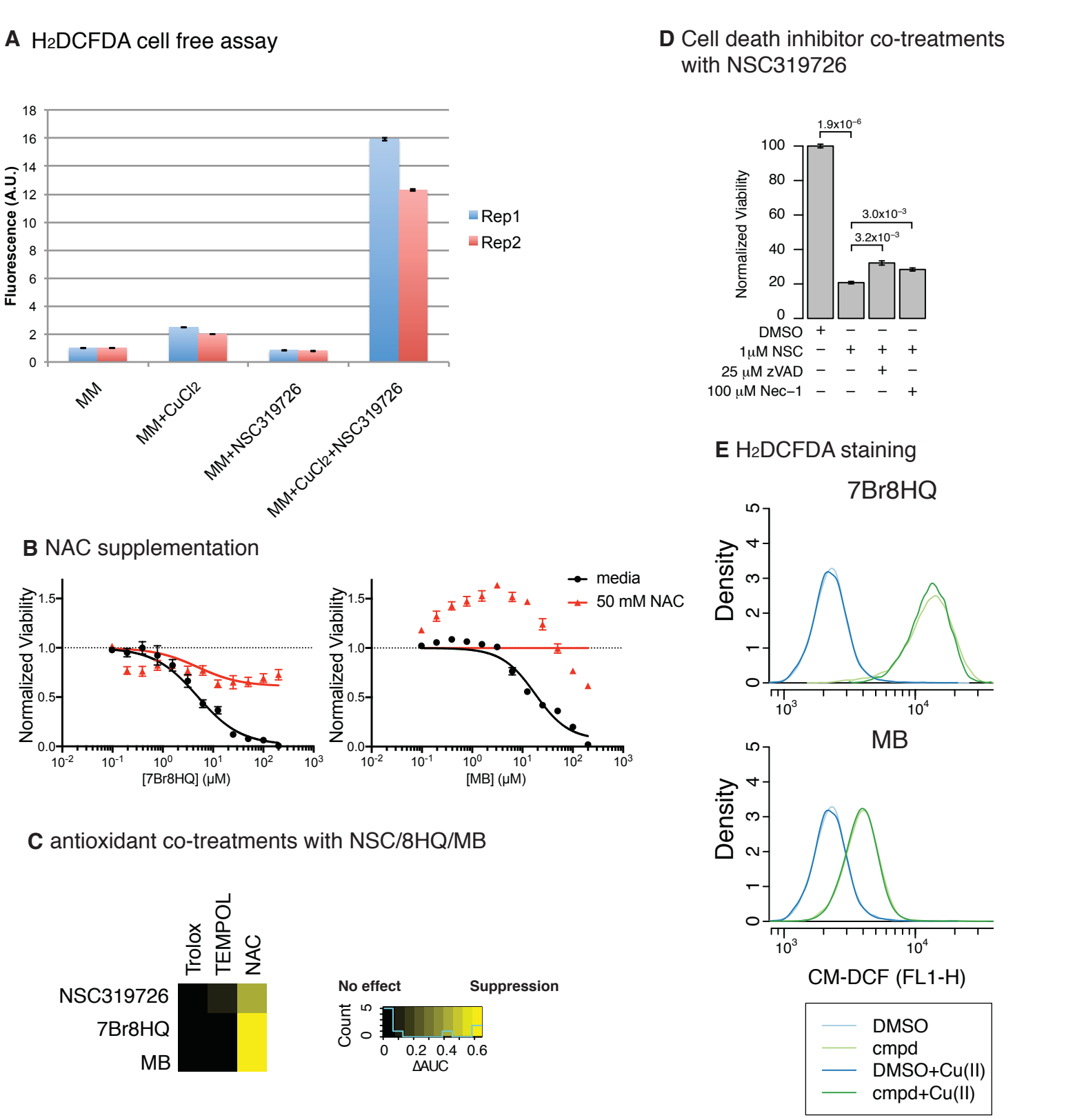

Figure S5. Three compounds, NSC319726/7Br8HQ/MB, and ROS generation, related to Figure 5. **A.** Production of DCF-detected ROS in cell free system. MM indicates master mixutre containing H2DCFDA + L-Cysteine + H2O2. **B-C.** 7Br8HQ and MB induced ROS generation. **B.** Effect of *N*-acetylcysteine on 7Br8HQ and MB lethality in HT-1080 cells. **C.** Effects of small panel of antioxidant (100 μM Trolox, 100μM TEMPOL (4-hydroxy TEMPO), 100mM NAC) on NSC319726/7Br8HQ/MB treatments tested in dilution series. Color code corresponds to the degree an antioxidant suppresses a lethal compound, which was assessed by $\Delta AUC = AUC_{M,L} - AUC_{L}$, where AUC indicates area-under dose-response curve of a lethal compound in HT-1080 cells, M and L indicate corresponding antioxidant and lethal compound, respectively. **D.** Effects of apoptosis (zVAD) and necroptosis (Nec-1) inhibitors on 1μM NSC319726 cytotoxicity. P-values from two-sided t-test are shown. **E.** CM-H2DCFDA staining of cells treated with DMSO/7Br8HQ/MB and media/Cu(II). **A, B,** and **D** indicate mean ± SEM of technical triplicates.

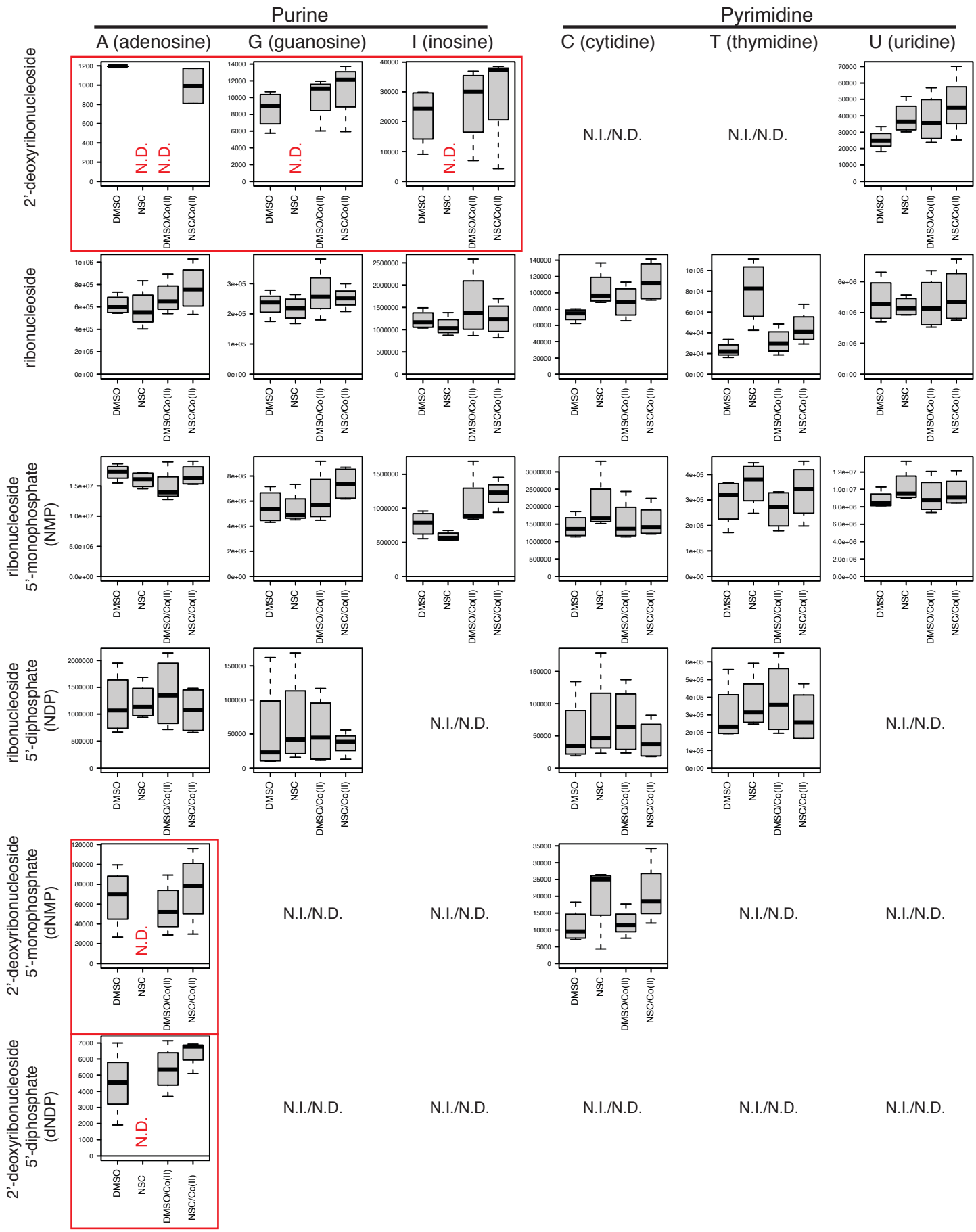

Figure S6. Quantification of purine/pyrimidine metabolites upon NSC treatment, related to Figure 5. A subset of untargeted metabolomic profiling showing purine and pyrimidine metabolites in HT-1080 cells. Each barplot summarizes biological quadruplicates of four conditions (0.1% DMSO, 5 μM NSC319726, DMSO/100 μM $CoCl_2$, 5 μM NSC319726/100 μM $CoCl_2$). Growth of HT-1080 cells was arrested when only NSC319726 was added and not on the other conditions. N.D.: not detected. N.I./N.D.: either not included in the metabolomic profiling from the beginning, or included but not detected because the quantity was too low in all four conditions.

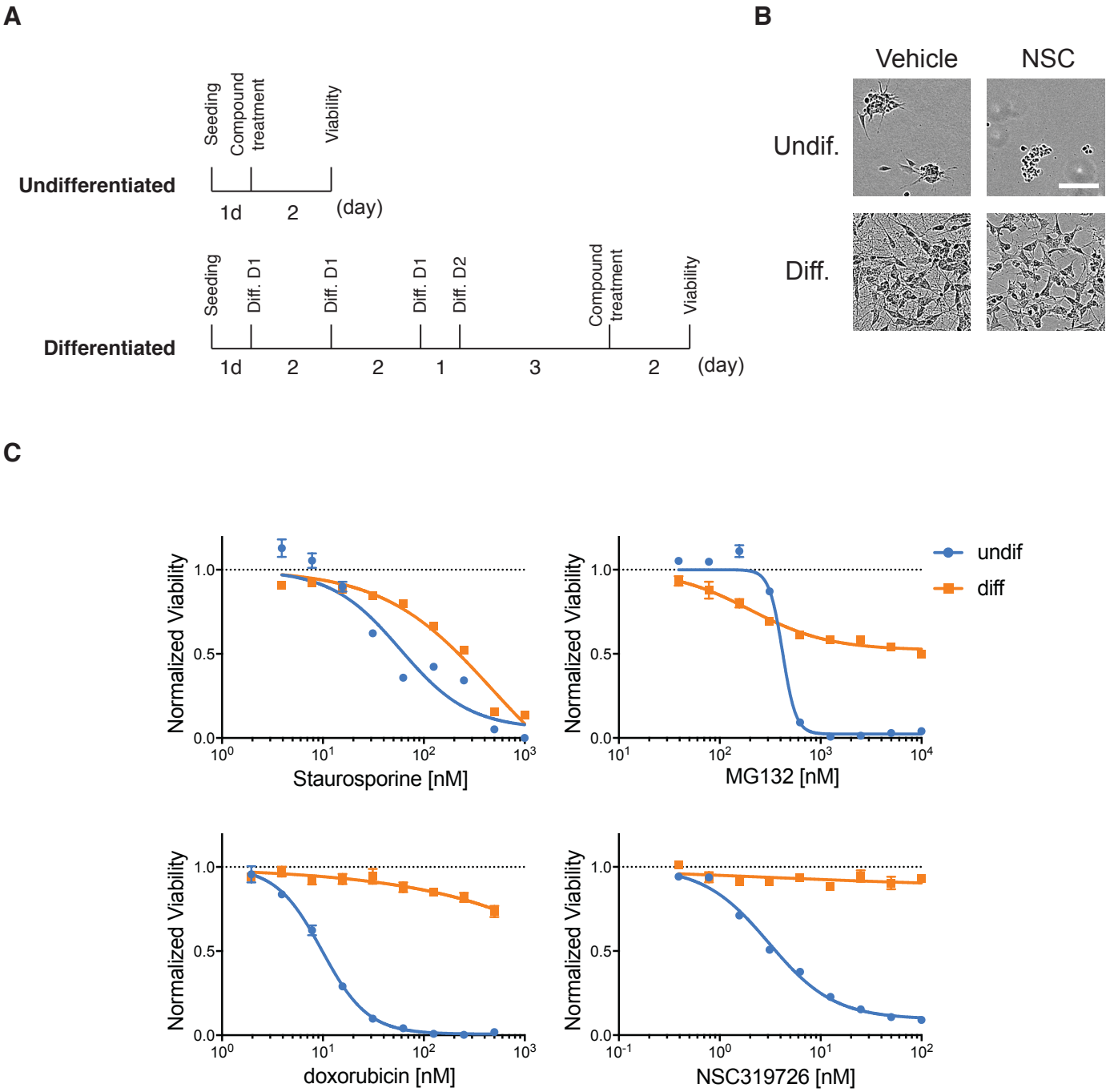

Figure S7. Neurotoxicity of four lethal compounds including NSC391726, related to Figure 5.
A. Scheme of neurotoxoxicity testing in undifferentiated and differentiated SH-SY5Y cells. **B.** Micrographs of SH-SY5Y cells treated with 1 μM NSC319726 or vehicle (0.1% DMSO) treatment. Scale bar is 100 μm. **C.** Dose-response curves of 9-points 2-fold dilution series of four lethal compounds in SH-SY5Y cells were shown. Experiments were performed in biological triplicates, and mean and SEM of the representative replicate were shown.